CFD-BASED PERFORMANCE EVALUATION OF THE AIR-SIDE HEAT TRANSFER ENHANCEMENT IN FAN-SUPPLIED TUBE-FIN EVAPORATORS

Jader R. Barbosa, Jr., jrb@polo.ufsc.br
Christian J. L. Hermes, hermes@polo.ufsc.br
Daniel S. Vieira[1]
Guilherme A. Dubiela[2]
POLO Research Laboratories for Emerging Technologies in Cooling and Thermophysics,
Department of Mechanical Engineering, Federal University of Santa Catarina, 88040-900 Florianopolis, SC, Brazil
[1] Presently at: Whirlpool S.A., Joinville, SC, Brazil
[2] Presently at: Petrobrás S.A., Santos, SP, Brazil

Abstract. *This paper performs a numerical analysis of the air-side convection heat transfer enhancement resulting from block-shaped protuberances placed on the fins of an evaporator commonly utilized in household refrigeration appliances. The effect of the number of vortex generators and their positioning relative to the tubes has been investigated. The fan performance curve has been incorporated into the heat transfer and pressure drop calculation methodology so that the effect of the enhanced fluid mixing on the air flow rate is properly accounted for. The present results, obtained assuming dry conditions (i.e., that condensate and frost deposition on the surface are negligible), show that an enhancement of the order of 6% of the heat transfer rate can be achieved, with the same fan, without a significant reduction of the air flow rate.*

Keywords*: tube-fin heat exchangers, heat transfer enhancement, vortex generation, fan curve, performance evaluation*

1. INTRODUCTION

In some compact tube-fin heat exchangers, enhancement of the air-side heat transfer performance is achieved using vortex generators placed on the fins. In comparison with other types of heat transfer enhancement techniques based on boundary-layer interruption and restart (i.e., offset-strip and louvered fins), vortex generation is often preferred due to the relatively lower increase of the air-side pressure drop resulting from the longitudinal vortices created downstream of the generator (Jacobi and Shah, 1995; Gentry and Jacobi, 1999).

The literature on heat transfer enhancement using vortex generation is extensive and a significant number of papers has been devoted to investigating in detail the fluid flow aspects of the problem, both experimentally and numerically. Fiebig *et al.* (1991) measured the flow losses and heat transfer coefficient resulting from delta wings, winglets and rectangular winglets distributed on flat fins. They found that the drag induced by the elements was proportional to the projected area and independent of the shape and Reynolds number. The observed local heat transfer augmentation was of several hundred percent with respect to the baseline (flat fin) configuration. Leu *et al.* (2004) carried out a numerical and experimental evaluation of block-shaped vortex generators mounted downstream of the tubes of a tube-fin heat exchanger. They found that the 45° inclination (between the block and the oncoming flow) provided the best heat transfer augmentation. Sohankar and Davidson (2003) solved numerically the flow and heat transfer in a plate-fin heat exchanger with vortex generators and found no significant differences between the velocity and temperature fields obtained with DNS and LES simulations. Khallaki *et al*. (2005) investigated numerically the formation and transport of longitudinal vortices generated by delta winglets using a commercial CFD package. They compared the results with experimental data and concluded that RSM and SST κ-ω models produced the more accurate predictions of the flow field and heat transfer. Dietz *et al.* (2006) conducted a numerical study of the vortex structures and their effect on the heat transfer in the wake of delta wing generators placed in line and side-by-side, also using a CFD package.

Despite the recent advances in the more fundamental understanding of the problem, there is a dearth in the literature regarding the incorporation of numerical simulations in design. In such cases, performance evaluation criteria (Webb and Kim, 2005) should be formulated in order to quantify the real enhancement potential of a given vortex generator configuration. In this sense, it is of utmost importance to consider the presence of the fan and the possibility of a reduction of the air flow rate due to an increase in pressure drop resulting from the addition of vortex generators on the fin surfaces.

The objective of this paper is to incorporate the CFD prediction of the heat transfer and pressure drop in enhanced heat exchangers into a calculation methodology that takes into account the influence of the fan. The study is based on the CFD calculation procedure of Barbosa *et al.* (2008), who put forward a methodology for simulating the air side of tube-fin evaporators commonly used as evaporators in *frost-free* household applications. Three configurations of enhanced fins with block-shaped vortex generators have been investigated. An enhancement of the order of 6% in the overall heat transfer rate was achieved with the best configuration without a significant reduction of the air flow rate produced by the fan.

2. MODELLING

2.1. Baseline geometry and boundary conditions

The basic dimensions of the heat exchangers evaluated in the present simulation are shown in Fig. (1). The width, *W*, height, *H*, and depth, *D*, are 305.0 mm, 59.6 mm and 192.0 mm, respectively. The outside diameter of the tubes is 8 mm and the number of tube rows is 10. The longitudinal and transverse tube pitches are 38.0 and 23.0 mm, respectively. The baseline simulations were carried out assuming 36 equally spaced 0.25 mm thick flat aluminium fins. The face velocities of the air stream were evaluated in the range between 0.47 m/s and 1.18 m/s. The inlet temperature of the air was set at 28ºC (301K) and the temperature of the outside tube wall was assumed uniform and equal to 32ºC (305K).

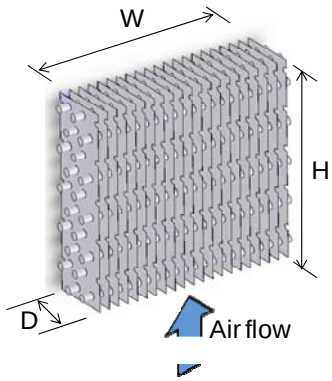

Figure 1. Basic geometry of the heat exchangers.

2.2. Mathematical formulation and implementation

The following assumptions have been adopted in the modeling of the fluid flow and heat transfer: (i) steady-state; (ii) newtonian fluid; (iii) incompressible flow; (iv) constant physical properties; (v) negligible body forces; (vi) no internal heat generation; (vii) turbulent flow; (viii) negligible radiation, viscous dissipation and buoyancy effects, and (ix) dry conditions (i.e., neither condensation nor frost formation). In the conservative form, the balance equations for mass, momentum, energy and turbulence quantities are as follows:

$$\nabla \cdot \vec{v} = 0 \tag{1}$$

$$\nabla \cdot \left(\rho \vec{v} \vec{v} \right) = -\nabla p + \nabla \cdot \left(\left(\mu + \mu_t \right) \left(\nabla \vec{v} + \nabla \vec{v}^T \right) \right) \tag{2}$$

$$\nabla \cdot \left(\vec{v} \left(\rho E + p \right) \right) = \nabla \cdot \left(\left(k + \frac{c_p \mu_t}{Pr_t} \right) \nabla T \right) \tag{3}$$

$$\nabla \cdot \left(\rho \vec{v} \kappa \right) = \nabla \cdot \left(\left(\mu + \frac{\mu_t}{\sigma_\kappa} \right) \nabla \kappa \right) + G_k + G_b - \rho \varepsilon - Y_m \tag{4}$$

$$\nabla \cdot \left(\rho \vec{v} \varepsilon \right) = \nabla \cdot \left(\left(\mu + \frac{\mu_t}{\sigma_\varepsilon} \right) \nabla \varepsilon \right) + \rho C_1 S \varepsilon - \rho C_2 \frac{\varepsilon^2}{\kappa + \sqrt{\nu \varepsilon}} + C_1 \frac{\varepsilon}{\kappa} C_3 G_b \tag{5}$$

The terms on the right hand side of Eqs. (4) and (5) are due to the production and destruction of κ and ε, and are described in detail by Shih *et al.* (1995). The turbulent viscosity and thermal conductivity are given by

$$\mu_t = \rho C_\mu \frac{\kappa^2}{\varepsilon} \tag{6}$$

$$k_t = \frac{c_p \mu_t}{Pr_t} \tag{7}$$

and the parameters and constants of the two-equation Realizable κ-ε Model (Eqs. 4-7) have been kept at the default values as proposed by Shih *et al.* (1995).

In this work, the governing equations have been integrated using a commercial CFD package (Fluent, 2005) based on the Finite Volume Method. The momentum and turbulence quantities equations have been discretized using the Power Law Scheme and the Second Order Upwind Scheme has been used to discretize the mass and energy equations (Versteeg and Malalasekera, 1995). The SIMPLEC algorithm (van Doormaal and Raithby, 1984) was employed in the pressure-velocity coupling, in which the pressure profile is calculated via the mass conservation equation. The convergence criterion for all balance equations was set at 10^{-4} RMS, the exception being the energy equation for which the convergence criterion was set at 10^{-6} RMS.

2.3. Validation of the solution procedure

Due to symmetry arguments, Barbosa *et al.* (2008) considered the flow and heat transfer on the air-side of the heat exchanger in a unit cell consisting of a half fin and a half discretized air channel adjacent to it. Here, the procedure outlined in Barbosa *et al.* (2008) for generating the computational grid and prescribing the boundary conditions in the simulation has been modified slightly to take into account the presence of the vortex generators on the surfaces of the fins. Two basic geometries of the baseline unit cell have been proposed and compared. In the first geometry ("fin-on-edges"), the discretized air channel is sided by two half fins (see Fig. 2). The 3D grid consists of approximately 400,000 hexahedrical 8-node elements with boundary conditions prescribed as follows: (i) uniform velocity and temperature prescribed at the channel inlet; (ii) pressure prescribed at the channel outlet; (iii) no-slip and known temperature specified at the tube walls and fins; and (iv) negligible thermal contact resistance between the fins and the tubes.

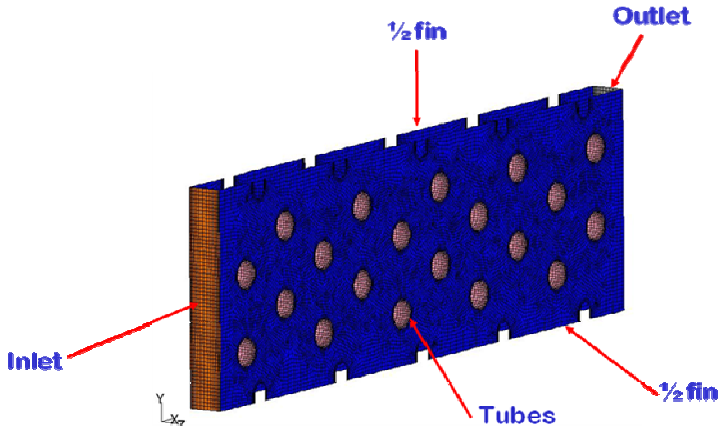

Figure 2. "Fin-on-edges" geometry.

The second geometry ("fin-in-middle"), shown in Fig. (3), consists of a fin sided by two discretized half air channels. This geometry has approximately the same number of grid elements with boundary conditions almost identical to the "fin-on-edges" geometry, except for the periodic boundary conditions applied on the symmetry plane corresponding to the air channels on each side of the fin. In both approaches, the Shell Conduction model available in the CFD package (Fluent, 2005) has been used to calculate the heat transfer in the fins. This reduced the total computational time and detailed analyses have demonstrated that it provides a very good approximation of the temperature field in the fin due to its small thickness and high thermal conductivity.

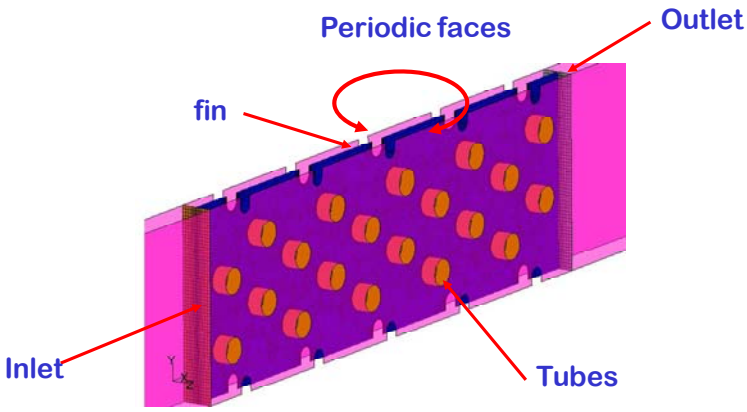

Figure 3. "Fin-in-middle" geometry.

Despite the fact that it has not been validated experimentally – as opposed to the "fin-on-edges" approach, which has been corroborated by experimental data in Barbosa *et al.* (2008) – the "fin-in-middle" configuration has a clear advantage over the "fin-on-edges" geometry for it is capable of handling fins which are non-symmetrical with respect to the *xy*-plane (see Fig. 3). In the present work, therefore, the "fin-in-middle" geometry was used in the simulations involving vortex generators placed on the fins. However, in order to guarantee that the configuration of the unit cell does not affect the nature of the results, a comparison between the two geometries using flat plain fins (baseline case) has been performed. Table (1) shows a comparison between the pressure drop and heat transfer capacity per unit cell calculated at two values of air face velocity for both configurations. As can be seen, the differences are negligible; indicating that the "fin-in-middle" approach is equivalent to the experimentally validated "fin-on-edges" configuration.

The pressure drop is calculated as the difference between the cross-section area average pressures at the inlet and outlet of the air stream and the heat transfer rate is calculated from an energy balance between the air inlet and outlet using mass flow average (mixing-cup) temperatures.

Table 1. Comparison between "fin-on-edges" and "fin-in-middle" configurations

Face velocity [m/s]	"fin-on-edges"		"fin-in-middle"		Difference	
	Δp [Pa]	Q [W]	Δp [Pa]	Q [W]	Δp [%]	Q [%]
0.47	13.159	2.234	13.147	2.233	0.094	0.045
1.18	2.469	1.048	2.469	1.047	-0.036	0.102

2.4. Geometry of the enhanced surfaces

Three vortex generator configurations have been investigated in the present work. The first and second configurations (VG1 and VG2) consist of 10 square protrusions embossed on the fins, as shown in Figs. (4.a) and (4.b). The blocks are in perfect alignment with the tubes, both in the longitudinal and transverse directions. Configurations VG1 and VG2 differ only with respect to the side of the fin on which the vortex generations are placed; in the VG1 case, all the elements are projected on one side of the fin, whereas in the VG2 geometry the elements stick out on each side of the fin. The third configuration (VG3) consists of 35 square elements protruding on both sides of the fins, as shown in Fig. (4.c). The dimensions of the cubic elements are the same for the three configurations (4 mm edge).

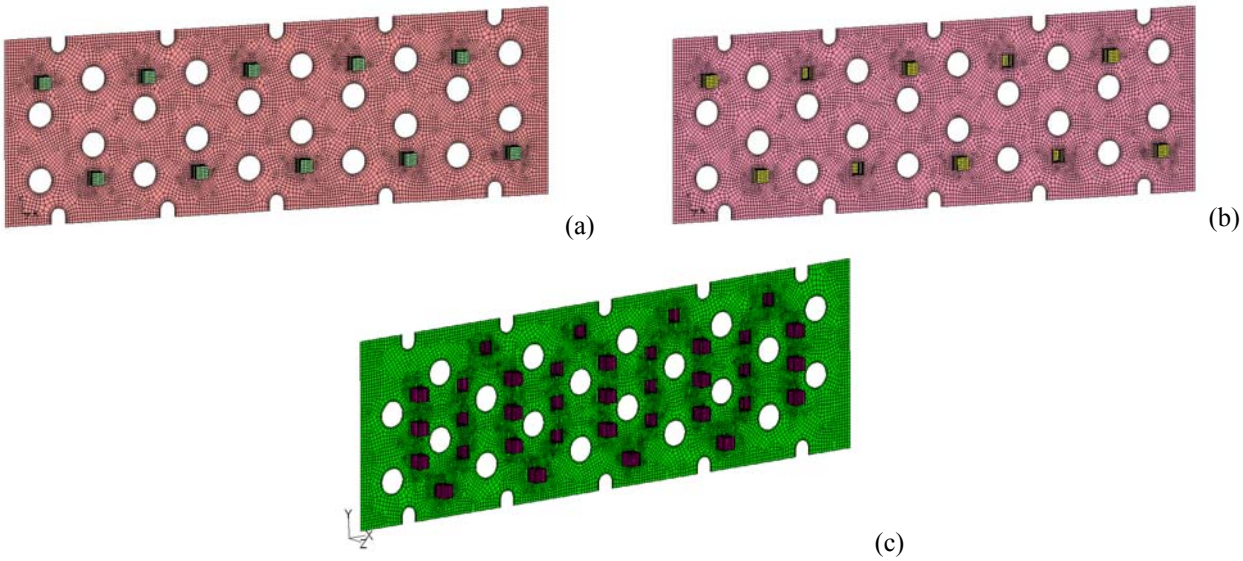

Figure 4. Configurations of the vortex generators. (a) VG1, (b) VG2, (c) VG3.

2.5. Performance evaluation criterion

The criterion adopted to evaluate the heat transfer enhancement associated with a specific fin configuration takes into account the influence of the air-side pressure drop on the air flow rate produced by the fan. In Fig. (5), the characteristic curve of the fan is plotted together with the system curves of three hypothetical heat exchangers with standard (St.), i.e. plain fins, and enhanced fin configurations (VGa and VGb). Because of the intrinsically higher pressure drops associated with the enhanced surfaces, the air flow rate experienced by the enhanced heat exchangers,

V_a and V_b, are lower than that of the standard case, V_{st}. The heat transfer rates given by the heat exchangers at the new points of operation are shown in Fig. (5.b), where only the fin configuration VGb can be considered as heat transfer enhanced (Q_b ! Q_{st}). Due to the excessive system pressure drop imposed by the geometry VGa, the air flow rate reduction was significant and, thus, impossible to be compensated by the higher heat transfer rates observed with configuration VGa *at a fixed flow rate*.

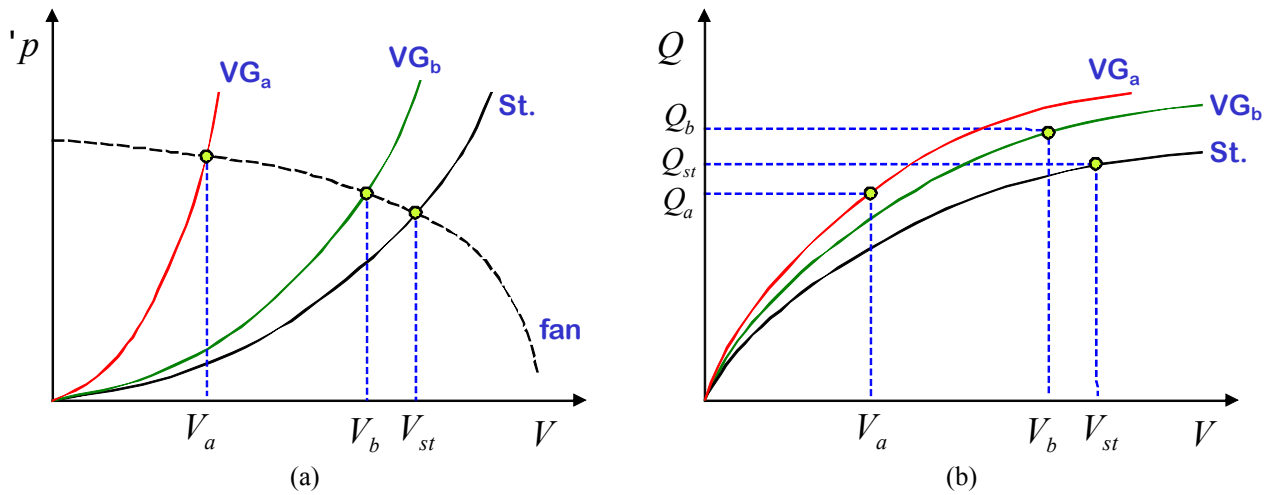

Figure 5. Illustration of the performance evaluation criterion

The following procedure was developed in order to determine the new point of operation and heat transfer rate associated with a potentially enhanced heat transfer surface:

1. CFD simulations were performed for the Standard (St.) and enhanced (VG1, VG2 and VG3) heat exchanger configurations – face velocities between 0.47 and 1.18 m/s – in order to obtain the air side pressure drop and heat transfer characteristic curves for each heat exchanger as a function of the air flow rate (polynomial fits);
2. The characteristic pressure drop curve of the heat exchanger originally in place in the refrigerator under study – obtained experimentally through the methodology developed by Waltrich (2008) – was subtracted from the total pressure drop curve associated with the air flow circuit through the compartments of a 440L top-mount refrigerator. The total pressure drop curve was obtained experimentally by the appliance manufacturer and is proprietary information. The resulting curve is, therefore, due to the overall flow impedance of the refrigerator and freezer cabinets *but* the evaporator;
3. It is hypothesized that the total pressure drop curve of the air circuit with any heat exchanger configuration evaluated via CFD is equal to flow impedance curve of the refrigerator and freezer cabinets but the evaporator *plus* the heat exchanger impedance curve obtained numerically;
4. By matching the characteristic curve of the fan (also made available by the appliance manufacturer) and the total flow impedance curve obtained in item 3 above, the air flow rate can be determined. In the present work, a spreadsheet was set up to calculate the air flow rate via a numerical solution of the polynomial equations;
5. The calculated air flow rate was then input into the heat transfer rate characteristic curve obtained in item 1 above.

3. RESULTS AND DISCUSSION

The distributions of fin temperature and air temperature and velocity on the symmetry plane between two adjacent fins are shown in Figs. (6) to (8) for geometries VG1, VG2 and VG3 for an air flow rate of 51 m^3/h (30 ft^3/min). The scales are in [K] and [m/s] for the temperature and velocity contours, respectively. As shown in Barbosa *et al.* (2008), a significant fraction of the air flow rate by-passes the tube bundle through the side clearances between the edges of the fins and the tubes, thus creating a stratification of the air temperature in the *y* direction. Although this effect is somewhat minimized by the presence of the defrosting heater coil, it should, in principle, be minimized in design because of the associated reduction in the heat exchanger effectiveness.

As far as the fin temperature distributions are concerned, a very similar behaviour is observed for the VG1 and VG2 geometries, indicating an almost identical heat transfer performance. On the other hand, lower fin temperatures are

observed in the VG3 case, which result from the enhanced fluid mixing generated by the greater number of vortex generators employed in this configuration.

The air side pressure drop, overall thermal conductance and heat exchanger effectiveness – defined in Eqs. (8) and (9) – are shown in Table 2 as a function of the air flow rate. As can be seen, the three quantities increase with the addition of vortex generators to the fins. The expected behaviour of increasing pressure drop and thermal conductance and decreasing heat exchanger effectiveness with flow rate is observed. The latter is also influenced by the by-pass fraction, which increases with the air flow rate (Barbosa *et al.*, 2008).

$$UA = \frac{Q}{\Delta T_{lm}} = \frac{Q}{T_{a,out} - T_{a,in}} \ln\left(\frac{T_w - T_{a,in}}{T_w - T_{a,out}}\right) \tag{8}$$

$$\varepsilon = \frac{T_{a,out} - T_{a,in}}{T_w - T_{a,in}} \tag{9}$$

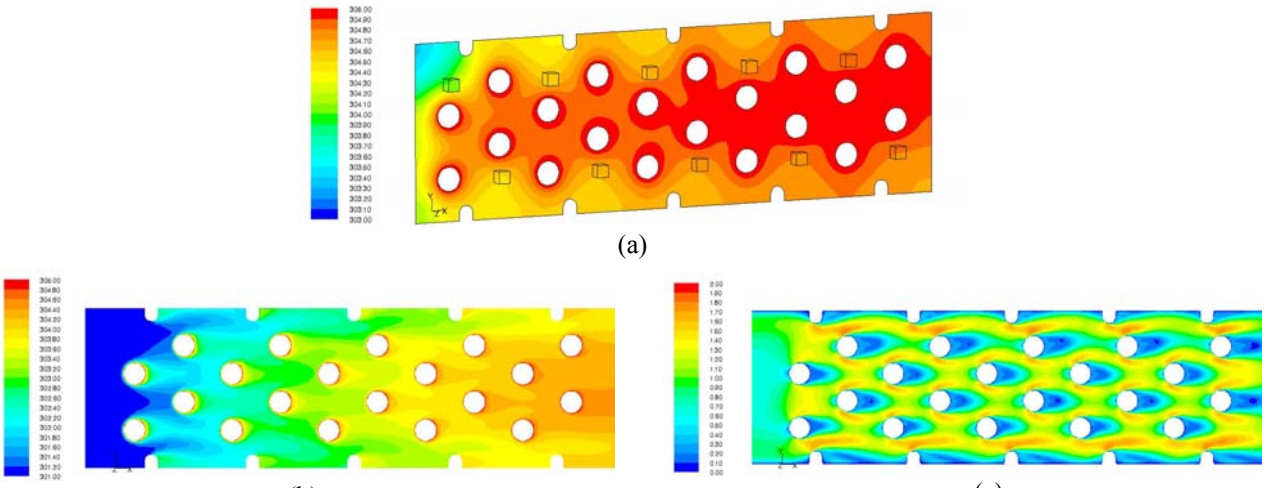

(a) (b) (c)

Figure 6. VG1 geometry, 51 m^3/h. (a) Fin temperature [K], (b) Air temperature [K], (c) Air velocity [m/s].

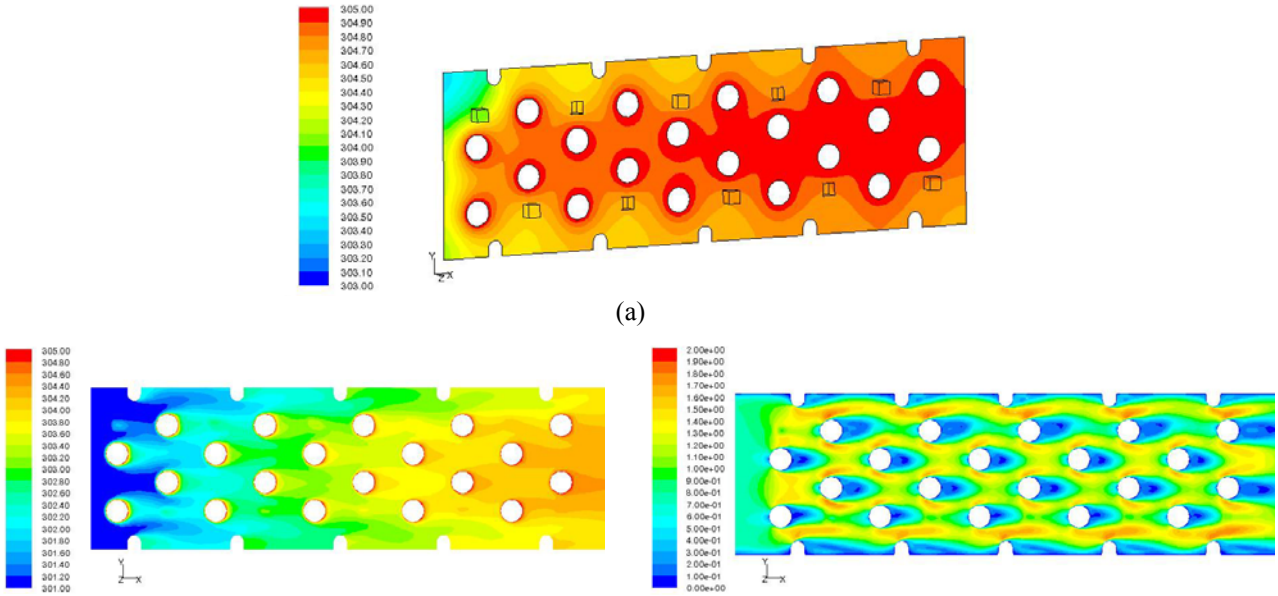

(a) (b) (c)

Figure 7. VG2 geometry, 51 m^3/h. (a) Fin temperature [K], (b) Air temperature [K], (c) Air velocity [m/s].

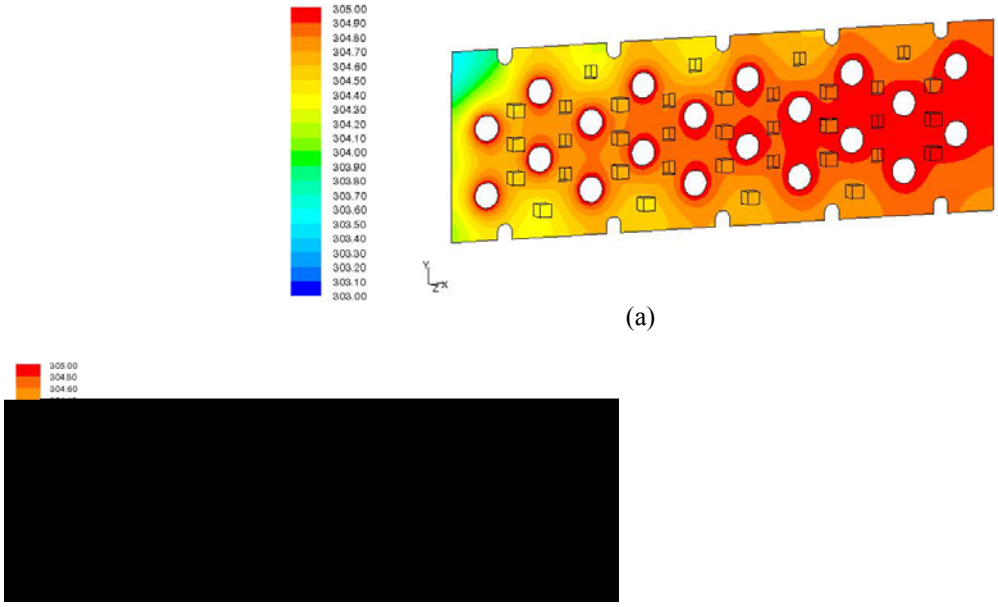

(a) (b) (c)

Figure 8. VG3 geometry, 51 m^3/h. (a) Fin temperature [K], (b) Air temperature [K], (c) Air velocity [m/s].

Table 2. Summary of the numerical simulation results.

Flow rate [m^3/h]	Standard			VG1			VG2			VG3		
	$'p$ [Pa]	UA [W/K]	ε	$'p$ [Pa]	UA [W/K]	ε	$'p$ [Pa]	UA [W/K]	ε	$'p$ [Pa]	UA [W/K]	ε
17	0.74	13.60	0.92	0.80	14.88	0.93	0.80	14.45	0.93	0.92	15.10	0.95
34	2.47	19.81	0.84	2.63	21.57	0.86	2.65	20.90	0.85	2.96	22.64	0.88
51	5.13	25.08	0.78	5.47	27.16	0.81	5.55	26.37	0.80	5.07	28.99	0.84
68	8.70	29.83	0.74	9.45	32.31	0.77	9.49	31.27	0.76	10.31	34.70	0.80
85	13.16	34.22	0.71	14.42	37.04	0.74	14.44	35.77	0.73	15.70	39.86	0.77

Table 3 shows the results of the performance evaluation criterion for heat transfer enhancement, considering the influence of the fan. It has been found that, for the fan in question, the air flow rate is only slightly sensitive to the increase in pressure drop due to the presence of the vortex generators. In this case, taking the Standard heat exchanger as the baseline configuration, all of the VG geometries would potentially enhance the heat transfer rate.

Table 3. Performance evaluation criterion results.

	Air flow rate [m^3/h]	Q [W]	Increase [%]
Standard	39.90	42.12	-
VG1	39.78	43.28	2.75
VG2	39.90	42.78	1.57
VG3	39.78	44.62	5.94

4. CONCLUSIONS

This paper presented a CFD study of the fluid flow and heat transfer in tube-fin heat exchangers with block-shaped vortex generators distributed over the continuous fins. Velocity and temperature distributions in the flowing air and fins have been presented to demonstrate the potential of the technique in the evaluation of flow mal-distributions and leakages through the side clearances (Barbosa *et al.*, 2008).

A performance evaluation criterion which incorporates the CFD calculations has been proposed to evaluate the heat transfer enhancement potential of a given fin configuration. This procedure takes into account the influence of the variation of the air-side pressure drop on the determination of the new flow rate produced by the fan. The finned surface can be considered as heat transfer enhanced if the heat transfer rate at the new flow rate is higher than that experienced with the original (baseline) fin surface. The criterion was demonstrated with three different enhanced fin configurations.